

# 东营凹陷永82井沙四段紫红色泥岩特征 及其在层序划分中的应用

张立强<sup>1</sup> 杨 晚<sup>2</sup> 侯冠群<sup>3</sup>

(1.中国石油大学(北京)地球科学学院,北京 102249;2.Missouri University of Science and Technology, Rolla Missouri 65409;3.成都理工大学 能源学院,四川 成都 610059)

**摘要** 在层序地层学研究中,层序界面的识别主要依据纵向分辨率较低的地震剖面、多解性较强的录井岩性组合和测井曲线等资料,而忽视了与不整合面有关的岩石古化学风化特征的分析,从而造成层序划分方案的多解性。通过对东营凹陷永82井沙四段紫红色泥岩的岩石学、地球化学以及古化学风化特征的分析,探讨了紫红色泥岩的纵向结构及其与层序界面的关系。永82井沙四段泥岩包括紫红色疏松状泥岩、紫红色致密块状泥岩、灰色层状泥岩以及灰色含膏泥岩和泥膏岩。沙四段紫红色疏松状泥岩具有强烈的擦痕面,其化学元素组成与古土壤相近,曾遭受程度较弱的古化学风化作用。结合紫红色泥岩的古化学风化特征认为,沙四段内部的层序界面与沙四段上、下亚段的边界不一致,紫红色疏松状泥岩段的顶界为沙四段内部的层序界面,而传统沙四段下亚段顶部的灰色砂岩夹紫色泥岩段属于上部层序的低水位体系域。

**关键词** 沙河街组 泥岩 地球化学特征 层序边界 古土壤 东营凹陷

中图分类号 :TE122.1

文献标识码 :A

文章编号 :1009-9603(2012)05-0043-04

层序界面的识别是层序地层学研究的重要内容。在层序地层学研究中,层序界面的识别主要依据地震剖面、录井岩性组合及测井曲线等资料所推测的不整合面或沉积间断面<sup>[1-7]</sup>,而针对不整合面及其结构的岩石学特征的研究则相对较少<sup>[8-9]</sup>。实践证明,地震剖面的纵向分辨率较低,而测井曲线和录井岩性组合具有多解性,因此造成不同学者对同一地区或同一目的层层序界面的识别存在较大差异,影响了层序界面的正确划分,成为层序格架建立中的一大难题。

在东营凹陷的油气勘探中,古近系沙河街组沙四段已成为其深层最主要的勘探目的层系。相对于浅层,由于地震剖面分辨率低,造成对其内部层序的划分及沉积体系的研究难度较大。前人对东营凹陷沙四段的层序划分存在较大差异<sup>[1-7]</sup>,主要依据岩性组合、电性和地震剖面特征,提出了许多不同的划分方案和观点。例如分别将沙四段划分为1个三级层序<sup>[2]</sup>、2个三级层序(分别对应于沙四段上亚段和下亚段)<sup>[3-4]</sup>、3个三级层序(分别对应于沙四段上、中、下亚段)<sup>[5]</sup>以及4个三级层序(沙四段上亚段和下亚段各划分为2个三级层序)<sup>[6-7]</sup>等。存在差

异的主要原因可能是对东营凹陷层序界面的识别及其特征认识的差异性造成的,此外,上述层序界面几乎与传统的岩石学地层单元的边界位置完全一致,而岩石学地层单元的边界往往具有穿时性<sup>[1]</sup>,因此对沙四段层序界面的等时性也需要进行深入研究。笔者在前人工作和认识的基础上,对沙四段紫红色泥岩的岩石学、地球化学及其古化学风化特征进行了探讨,以期对沙四段层序界面的划分依据进行补充。

## 1 区域地质概况

东营凹陷位于济阳拗陷南部,其北邻陈家庄凸起和滨县凸起,西接林樊家低凸起和青城凸起,向南超覆于鲁西隆起和广饶凸起,向东以沂沭大断裂为界,为北断南超的新生代箕状断陷沉积盆地<sup>[1-2]</sup>。东营凹陷古近系和新近系自下而上发育孔店组、沙河街组、东营组、馆陶组、明化镇组和平原组<sup>[1]</sup>,其中沙河街组是其最重要的勘探目的层系,可分为沙四段、沙三段、沙二段和沙一段。根据岩性特征,沙四段(岩石学地层单元)可进一步划分为下亚段( $E_{S4}^F$ )

收稿日期 2012-07-10。

作者简介 张立强,男,教授,博士,从事储层地质学及层序地层学研究。联系电话:18678986578, E-mail: liqiangzhangwxm@163.com。

基金项目 国家油气科技重大专项 东营凹陷北带中段深层沉积充填历史及砂岩富集带分布规律研究(2011ZX05008-004-52)。

和上亚段( $E_{s4}^+$ ) ,沙四段下亚段和上亚段的传统划分标准是当紫红色泥岩出现时即划为下亚段。 $E_{s4}^+$ 的岩性为紫红色泥岩夹棕色、棕褐色粉砂岩、砂质泥岩和薄层碳酸盐岩, $E_{s4}^+$ 的岩性主要为灰色、深灰色、灰褐色湖相泥岩夹碳酸盐岩、砂岩及油页岩。在东营凹陷的不同构造部位,其岩性存在一定的差异,其中凹陷中部主要发育盐岩和石膏层,陡坡带主要发育砂砾岩体,缓坡带发育灰岩和白云岩,洼陷带发育泥岩、泥灰岩及油页岩等;自下而上,整体呈现粗 细 粗的完整旋回或粗 细的正旋回<sup>[1]</sup>。

## 2 岩石学特征

对东营凹陷东北部永安镇地区永82井的紫红色泥岩的研究结果表明,其沙四段下亚段发育冲积平原及滨浅湖相沉积,岩性以紫红色泥岩和粉砂质泥岩为主,夹灰色石膏结核层、灰绿色泥岩及粉砂质泥岩。永82井第1和第2次取心的层位为沙四段下亚段上部,埋深为2 549~2 565 m。

根据取心井段岩石的颜色、结构及构造不同,将永82井钻遇的泥岩分为4种类型:①紫红色疏松状泥岩,该类泥岩固结程度较差,沉积层理不发育;具有强烈的擦痕面,且擦痕面光滑、呈油脂光泽(图1a),存在零星分散的石英和长石颗粒,镜下观察,泥岩中存在块状方解石微晶,代表碳酸盐结核的发育早期,具有古土壤的沉积特征<sup>[10-11]</sup>。②紫红色致密块状泥岩,该类泥岩的内部均质、层理不发育,呈致密块状,与疏松状泥岩相比,其擦痕面不发育,为成岩和压实作用较强的氧化环境下形成的正常泥岩沉积(图1b)。③灰色层状泥岩,该类泥岩的颜色为深灰、灰绿或灰色,见不连续纹层,呈致密层状(图1c)。④灰色含膏泥岩和泥膏岩,其颜色以灰色、灰绿色为主,含结核状或透镜状石膏团块(图1d)。

垂向上,永82井取心井段的岩性及颜色呈规律性变化,共组成4个韵律。在每个韵律内,自下而上,泥岩颜色一般由灰绿色、灰紫色到紫红色;岩性

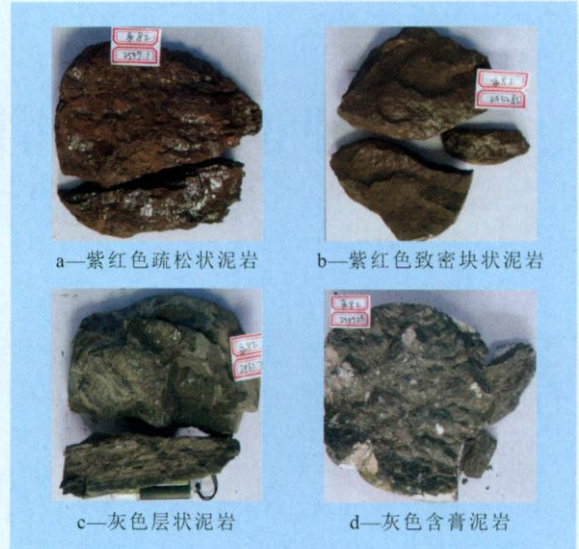


图1 永82井沙四段典型泥岩类型

由灰色层状泥岩、灰色含膏泥岩、泥膏岩变为紫红色致密块状泥岩、紫红色疏松状泥岩;沉积构造由层理发育到致密块状,最后变为疏松状。

通过X-衍射全岩分析发现,紫红色疏松状泥岩以粘土矿物为主,其含量为46%~54%;其次为石英、斜长石、方解石和赤铁矿,其含量分别为19%~20%,8%~9%,11%~15%和4%~5%;不含钾长石。紫红色致密块状泥岩和灰色层状泥岩的粘土矿物和赤铁矿的含量相对较低,分别为30%~44%和0~4%,钾长石的含量较高,为5%~9%。灰色含膏泥岩和泥膏岩的粘土矿物、石英及长石的含量均较低;硬石膏的含量较高,为40%~65%;含少量的菱铁矿和黄铁矿,其含量均为1%~2%。

## 3 地球化学特征

对永82井取心井段的紫红色疏松状泥岩和紫红色致密块状泥岩等样品进行常量元素分析(表1),结果表明,紫红色疏松状泥岩或紫红色致密块状泥岩的不同样品中常量元素的含量较为相近,其中紫红色疏松状泥岩样品的 $SiO_2$ 、 $Al_2O_3$ 、CaO和MgO

表1 永82井沙四段取心井段泥岩与不同类型泥岩对比

| 样品类型                  | 化学蚀变指数      | $SiO_2$ 含量 | $Al_2O_3$ 含量 | CaO含量     | MgO含量   | $K_2O$ 含量 | $Na_2O$ 含量 | $Fe_2O_3$ 含量 | MnO含量     | % |
|-----------------------|-------------|------------|--------------|-----------|---------|-----------|------------|--------------|-----------|---|
| 紫红色疏松状泥岩              | 60.4~62.9   | 45.9~47.3  | 16.15~16.8   | 4.67~5.77 | 3.7~4.8 | 3.3~3.9   | 1.3~1.4    | 7.4~8        | 0.07~0.14 |   |
| 紫红色致密块状泥岩             | 58.1~61.5   | 51.6~54.4  | 16.8~18      | 4.91~7.31 | 3.1~4.2 | 3.9~4.1   | 1.5~1.7    | 5.5~8.5      | 0.06~0.11 |   |
| 灰色泥岩                  | 57.4        | 47.4       | 16.55        | 7.34      | 3.39    | 3.36      | 1.57       | 5.24         | 0.11      |   |
| 上部陆壳 <sup>[12]</sup>  |             | 62.4       | 18.88        | 1.29      | 2.19    | 3.68      | 1.19       | 7.18         |           |   |
| 古土壤 <sup>[13]</sup>   | 65.99~69.71 | 52         | 16           | 2.6       | 0.6     | 0.8       | 1.9        |              |           |   |
| 西峰红粘土 <sup>[14]</sup> |             | 50.87      | 11.84        | 10.97     | 2.89    | 2.24      | 1.03       | 3.69         | 0.08      |   |

的含量分别为 45.9% ~ 47.3% ,16.15% ~ 16.8% , 4.67% ~ 5.77%和 3.7% ~ 4.8%。不同类型泥岩样品的化学元素含量差异较大,以紫红色疏松状泥岩与灰色泥岩之间的差异最大。

研究表明,永82井取心井段紫红色疏松状泥岩的化学元素组成与上部陆壳<sup>[12]</sup>存在明显差异,而与一般古土壤<sup>[13]</sup>相近。与上部陆壳的化学元素组成对比结果表明,研究区紫红色疏松状泥岩的SiO<sub>2</sub>和Al<sub>2</sub>O<sub>3</sub>的含量较低,分别比上部陆壳的低15.1% ~ 16.5%和2.08% ~ 2.73%;而CaO、MgO和Na<sub>2</sub>O的含量较高,其中CaO和MgO的含量分别比上部陆壳的高3.38% ~ 4.48%和1.51% ~ 2.61%。与古土壤<sup>[13]</sup>的

化学元素组成对比结果表明,其SiO<sub>2</sub>、Al<sub>2</sub>O<sub>3</sub>和Na<sub>2</sub>O的含量基本相近,但研究区紫红色疏松状泥岩的CaO、MgO和K<sub>2</sub>O的含量相对较高,均比古土壤的高约2% ~ 4%。与甘肃西峰晚新近纪红粘土<sup>[14]</sup>的化学元素组成对比结果表明,研究区紫红色疏松状泥岩的Al<sub>2</sub>O<sub>3</sub>、Fe<sub>2</sub>O<sub>3</sub>、MgO和K<sub>2</sub>O的含量较高,其中Al<sub>2</sub>O<sub>3</sub>和MgO的含量分别比甘肃西峰晚新近纪红粘土的高4.31% ~ 4.96%和0.81% ~ 1.91%,而SiO<sub>2</sub>和Na<sub>2</sub>O的含量则较为接近(表1)。

纵向上,研究区Fe<sub>2</sub>O<sub>3</sub>和MgO的含量自上而下逐渐降低,而Na<sub>2</sub>O和CaO的含量则呈逐渐增加的趋势(图2),表明研究区可能受到风化或成壤作用的影响。

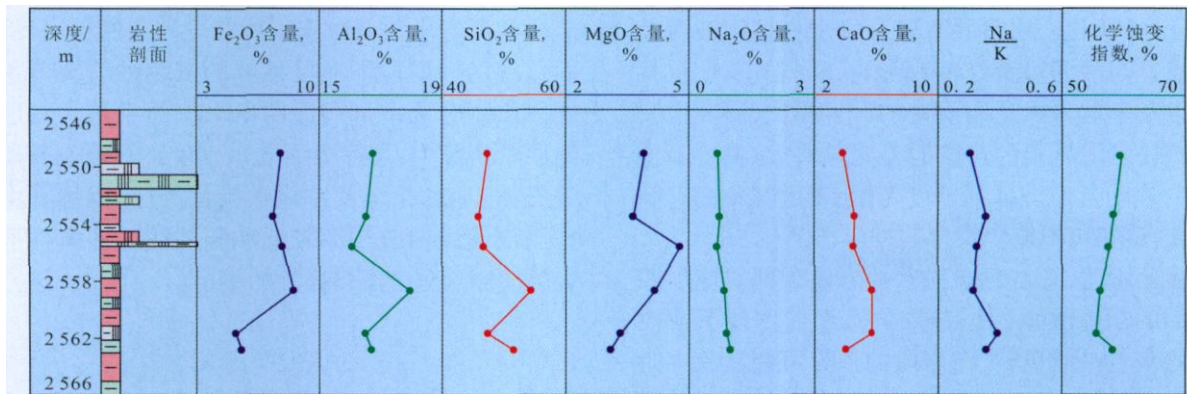


图2 永82井取心井段泥岩的化学元素组成及化学蚀变指数变化

影响,岩石中易风化矿物遭受破坏,造成抗风化能力强的微量元素在近地表相对富集,以及易溶解化学成分流失而难溶解化学成分富集。

## 4 古化学风化特征及其在层序划分中的应用

### 4.1 古化学风化特征

化学风化是表生环境中主要的地质作用之一,常利用化学蚀变指数<sup>[15-16]</sup>、钠钾比值(Na/K)<sup>[13]</sup>和铷锶比值<sup>[13]</sup>等来研究沉积物所受的化学风化程度。其中化学蚀变指数是评估古化学风化程度的参数,也是定量评价长石向粘土转化程度的重要参数,被广泛应用于确定岩石的古化学风化程度及其风化差异性评价的研究中<sup>[16]</sup>。一般来说,由于化学蚀变指数的计算方法对CaO含量较高样品的化学风化程度的估算过低,因此通常要求在计算过程中去除CaO含量大于10%的样品<sup>[17]</sup>。研究表明,岩石的古化学风化程度越强,其化学蚀变指数越大。

永82井沙四段上亚段紫红色泥岩样品的化学蚀变指数的计算结果(表1)为58.1% ~ 62.9%,接近于古土壤的化学蚀变指数(65.99% ~ 69.71%)<sup>[13]</sup>,但

低于残积粘土(化学蚀变指数为85% ~ 100%)<sup>[15]</sup>。说明紫红色泥岩处于不整合面之下的半风化岩层带,曾遭受相对较弱的古化学风化作用<sup>[15]</sup>,且永82井紫红色泥岩样品的化学蚀变指数自上而下呈逐渐降低的趋势(图2),说明其古化学风化程度随着埋深增大而逐渐减弱。

钠钾比值也是衡量岩石古化学风化程度的指标<sup>[13]</sup>,可用于表征岩石中斜长石的古化学风化程度。由于斜长石的风化速率大于钾长石,因此岩石的钠钾比值与其古化学风化程度成反比。研究区紫红色疏松状泥岩钠钾比值变化与化学蚀变指数的变化特征相反,随埋深的增加,钠钾比值具有逐渐增大的趋势(图2),反映出紫红色疏松状泥岩段曾遭受古化学风化作用,且风化程度随埋深增大而逐渐减弱。

### 4.2 层序界面的确定

根据紫红色泥岩的岩石学、地球化学及古化学风化特征,结合测井曲线特征,将永82井沙四段2500 ~ 2590 m井段自上而下划分为不整合面之上岩层带、风化粘土层带、半风化岩层带和未风化岩层带。其中,2500 ~ 2540 m井段为滨浅湖相沉积,以灰色砂岩及泥岩为主,夹紫色泥岩,为不整合面

之上岩层带,2 540~2 546 m井段为研究区处于暴露背景下,长期遭受剥蚀形成的不整合顶部的风化粘土层带,2 546~2 580 m井段为半风化岩层带,是由于地壳的频繁升降,研究区处于沉积与剥蚀作用交互的背景下,紫红色疏松状泥岩段代表短暂沉积间断和风化淋滤,灰色层状泥岩段代表正常浅水沉积,二者交互形成了不整合面之下的半风化岩层带,2 580~2 590 m井段以灰色泥岩及砂岩沉积为主,为未风化岩层带。

在电性上,风化粘土层带具有低密度、高声波时差和较低自然伽马的特点,半风化岩层带具有低密度、高声波时差,且存在声波时差曲线明显跳跃的特征,未风化岩层带具有较高密度和低声波时差的特点。与沙四段紫红色致密块状泥岩、灰色层状泥岩以及下覆未风化岩层带的泥岩相比,研究区紫红色疏松状泥岩段的声波时差明显增大、密度降低(图3),表明其声波传播速度变慢、密度减小而孔隙度增大,反映出不整合发育的特征<sup>[18]</sup>。

综上所述,紫红色疏松状泥岩段顶部对应沙四段内部的层序界面,具有等时性,而沙四段下亚段顶部的灰色夹紫色砂、泥岩段的顶界可能具有穿时性,传统的沙四段下亚段顶部的灰色砂岩夹紫色泥岩段应划为上部(A)层序的低水位体系域(图3)。

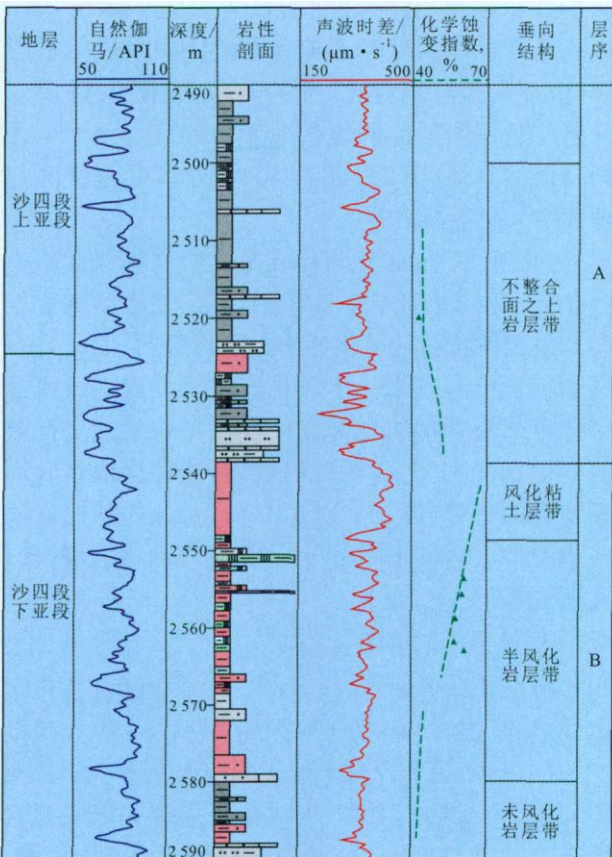


图3 永82井沙四段电性特征及层序划分

## 5 结束语

将东营凹陷永82井沙四段下亚段泥岩划分为紫红色疏松状泥岩、紫红色致密块状泥岩、灰色层状泥岩以及灰色含膏泥岩和泥膏岩共4种类型。紫红色疏松状泥岩具有强烈的擦痕面,其化学元素组成与古土壤的化学元素组成相近。结合泥岩的化学蚀变指数分析表明,紫红色疏松状泥岩曾遭受程度较弱的古化学风化作用,且其风化程度随埋深的增大而逐渐减弱。层序界面与传统岩石地层单元的边界不完全一致,研究区沙四段下亚段紫红色疏松状泥岩段顶部对应于沙四段内部的层序界面,而传统的沙四段下亚段顶部的灰色砂岩夹紫色泥岩段应划分为上部层序的低水位体系域。在层序地层学研究中,层序界面的识别应结合取心井段的岩石学、地球化学及古化学风化特征,以弥补由于地震剖面纵向分辨率较低和测井曲线多解性而造成的层序划分方案多样性的不足。

### 参考文献:

[1] 纪友亮,张世奇,陆相断陷湖盆层序地层学[M].北京:石油工业出版社,1996.

[2] 武法东,陈建渝.东营凹陷第三纪层序地层格架及沉积体系类型[J].现代地质,1998,12(4):559-565.

[3] 冯有良.东营凹陷下第三系层序地层格架及盆地充填模式[J].地球科学-中国地质大学学报,1999,24(6):635-642.

[4] 隋风贵,赵乐强.济阳拗陷不整合结构类型及控藏作用[J].大地构造与成矿学,2006,30(2):161-167.

[5] 李阳,蔡进功,刘建民.东营凹陷下第三系高分辨率层序地层研究[J].沉积学报,2002,20(2):210-216.

[6] 宋国奇,纪友亮,赵俊青.不同级别层序界面及体系域的含油性[J].石油勘探与开发,2003,30(3):32-35.

[7] 宋国奇.济阳拗陷下第三系湖相沉积的层序地层学分析[J].现代地质,1993,7(1):7-13.

[8] 陈涛,蒋有录,宋国奇,等.济阳拗陷不整合结构的发育过程及发育模式[J].油气地质与采收率,2009,16(5):33-36.

[9] 高永进.砂砾岩体沉积旋回划分及对比方法-以济阳拗陷盐家地区沙四段上亚段为例[J].油气地质与采收率,2010,17(6):6-11.

[10] 周自立,郝运轻,滕建彬,等.古土壤储层在胜利油区沙四段的发现[J].油气地质与采收率,2009,16(5):1-3.

[11] Yang Wan, Feng Qiao, Liu Yiqun, et al. Depositional environments and cyclo- and chronostratigraphy of uppermost Carboniferous-lower Triassic fluvial-lacustrine deposits, southern Bogeda mountains, NW China—a terrestrial paleoclimatic record of mid-latitude NE Pangea [J]. Global and Planetary Change, 2010,

(下转第53页)

的校正(图6),深度预测精度大幅度提高,白云凹陷参与速度场建立的22口井 $T_{50}$ 反射层深度误差为6~11 m,预留的B19和B20井实际钻井深度与时深转换得到的深度相比, $T_{50}$ 反射层深度误差分别为6和7 m,能够满足海洋深水区油气勘探的需求。

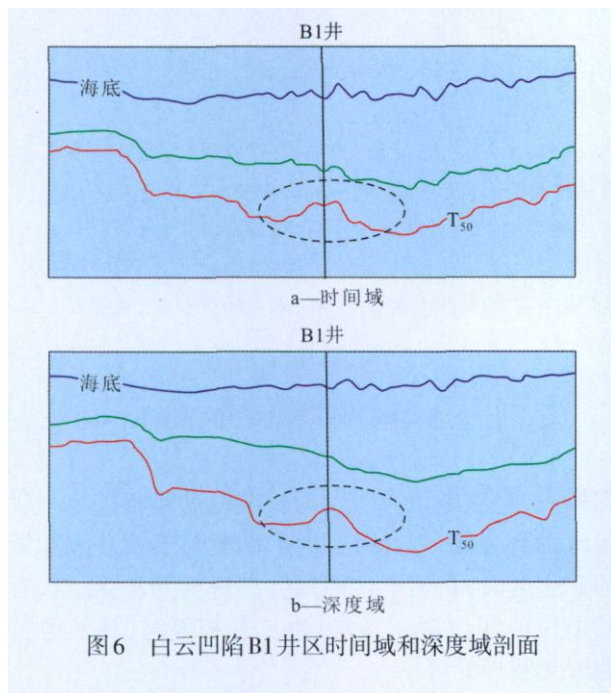


图6 白云凹陷B1井区时间域和深度域剖面

### 3 结束语

地层速度随海水深度增加而降低只是表面现象,地层速度与海水深度不存在必然的联系,陆架坡折带是界定地层速度异常的关键,沉积环境的差别是陆坡深水区速度异常的根本原因。双层模型法将海水层和沉积层剥离分析,可以较好地消除海水对地层平均速度的影响,测井速度、地震叠加速

度和叠前相干速度反演的有机结合,是建立海洋深水区速度场较为有效的方法。

#### 参考文献:

- [1] 李伍志,王璞珺,张功成.珠江口盆地深部基底地层的地震时深转换研究[J].地球物理学报,2011,54(2):449-456.
- [2] 何敏,朱明,汪瑞良.白云深水崎岖海底区时深转换方法探讨[J].地球物理学进展,2007,22(3):966-971.
- [3] 李杏莉,王彦春.不同基准面上的速度场及时深转换[J].物探与化探,2008,33(1):49-53.
- [4] 马涛,严又生,刘文利.塔里木盆地速度场的建立及应用[J].石油地球物理勘探,1996,31(3):382-393.
- [5] 武学明,张勇军.一种由叠加速度转换为平均速度的方法[J].地球物理学报,2008,51(8):50-53.
- [6] 韩宏伟,崔红庄,赵海华,等.三维速度场建立方法[J].油气地质与采收率,2010,17(1):54-56,61.
- [7] 韩小俊,韩波.塔里木盆地库车坳陷中部地震速度场的建立方法[J].天然气工业,2009,29(12):23-25.
- [8] 谢锐杰,朱广生,漆家福.声波测井资料在平均速度场中的应用[J].西南石油学院学报,2003,25(1):9-11.
- [9] 尚延安.塔里木盆地轮南地区速度场的建立和应用[J].油气地质与采收率,2008,15(4):49-51.
- [10] 曾驿,汪瑞良,刘从印.变速成图技术在番禺4注低幅构造研究中的应用[J].内蒙古石油化工,2010,47(4):117-119.
- [11] 冯全雄,黄兆林,葛勇.模型研究指导层速度解释方法探索及应用[J].中国海上油气,2005,17(3):171-178.
- [12] 吴清岭,李来林,李慧.约束速度反演在大庆油田复杂构造成像中的应用[J].大庆石油地质与开发,2009,28(5):295-298.
- [13] 张玉芬.测井资料约束的层速度反演[J].石油与天然气地质,1998,19(3):227-231.
- [14] 王天禧.石油地震勘探数据叠前速度反演稳定性初步分析[J].中国海上油气地质,1998,12(3):206-209.

编辑 经雅丽

#### (上接第46页)

- 73(1/2):15-113.
- [12] Taylor S R, McLennan S M. The continental crust: its composition and evolution[M]. Oxford: Blackwell Publishing, 1985: 1-312.
- [13] Bestland E A. Alluvial terraces and paleosols as indicators of early Oligocene climate change (John Day Formation, Oregon)[J]. Journal of Sedimentary Research, 1997, 67(5): 840-855.
- [14] 陈晔, 陈骏, 刘连文. 甘肃西峰晚第三纪红粘土的化学组成及化学风化特征[J]. 地质力学学报, 2001, 7(2): 167-175.
- [15] Nesbitt H W, Young G M. Early Proterozoic climates and plate motions inferred from major element chemistry of lutites [J]. Nature, 1982, 299 (21): 715-717.
- [16] Sheldon N D, Retallack G J, Tanaka S. Geochemical climofunctions from North America soils and application to paleosols across the Eocene-Oligocene boundary in Oregon [J]. Journal of Geology, 2002, 110(6): 687-696.
- [17] Girty G H, Ridge D L, Knaack C. Provenance and depositional setting of Paleozoic chert and argillite, Sierra Nevada, California [J]. Journal of Sedimentary Research, 1996, 66(1): 107-118.
- [18] 张立强, 罗晓容, 何登发, 等. 准噶尔盆地南缘下白垩统层序界面的识别[J]. 沉积学报, 2004, 22(4): 636-642.

编辑 邹淑滢

300452, China

**Wu Changwu, Xiong Liping, Huang Yanqing. Hydrocarbon distribution and control factors on accumulation in Bonaparte basin. *PGRE*, 2012, 19(5):31–33.**

**Abstract:** Bonaparte basin is a gas prone basin in which Sinopec hold 3 blocks interests. It baffled blocks exploration and development efficiently of these existing blocks and the acquisition of new blocks that the main control factors of hydrocarbon accumulation and potential are not so clear. The author points out the main control factors of hydrocarbon accumulation and the potential of Bonaparte basin through the research of petroleum geology and the hydrocarbon distribution. Hydrocarbon dose unequally distribute in this basin, the west part of basin is mainly small and medium oil fields but the east part of basin mainly contains giant gas fields. The kerogen type, maturity and preservation condition determined hydrocarbon type. In the west part of basin, the reactivation of faults leads to the lost of hydrocarbon and the scale of oil fields is small. But, in the east part of basin, the structure reinforced in late Miocene leads to the gas fields grow giant. Sub-basins in this basin have different main control factor of oil-gas accumulation. Preservation condition is the main control factor of oil-gas accumulation of Vulcan sub-basin, for the Calder Garben, the main control factor is the reservoir quality, and the trap is the main control factor of the east slope of the basin. Bonaparte basin still has good potential for exploration especially in medium and small structural traps, faults related traps, lithologic traps and salt related traps.

**Key words:** oil & gas distribution character; main control factor of oil-gas accumulation; source rock; preservation condition; reservoir quality; trap condition; Bonaparte basin

**Wu Changwu,** Petroleum Exploration and Production Research Institute, SINOPEC, Beijing City, 100083, China

**Yu Jianghao, Liao Yuantao, Lin Zhengliang et al. Research on temporal diversity of settlement characteristics of Paleogene, Fushan Sag. *PGRE*, 2012, 19(5):34–38.**

**Abstract:** Tectonic is very active in Cenozoic of Beibuwan Basin, Fushan Sag located in margin of Beibuwan Basin, whose regional tectonic of Paleogene is very complicated and research level is low, without study of tectonic subsidence history. Application of EBM basin modeling system for subsidence history in Fushan Sag, the back stripping analysis shows that: Fushan Sag has successively suffered rift period, transformational period and depression period, the changing of subsidence rate emerges “episode” characteristic; west secondary depression sedimentation rate is higher than which in east secondary depression since chasmic I episodic period, but from the chasmic III episodic, the east secondary depression sedimentation increased, so, the sedimentation rate is higher than which in west secondary depression. From the location of the center of subsidence, at the early period of chasmic, the subsidence center is located in the Huang Tong region of western depression, but at the advanced of chasmic (chasmic III episodic), the center of subsidence gradually migrates to the Bailian region of eastern depression, then, the regional center of subsidence continues migration to the northeast. Vertical sedimentation rates of the east and west secondary depression are different, besides, regional subsidence center migrates from west to east of Paleogene in Fushan Sag, reflecting the east and west secondary depression in Fushan Sag having space-time diversity in the characteristics of subsidence; Research finds that the tectonic activity diversity of secondary depression and Fushan Sag suffered by regional asymmetric extension effect is inner mechanism which has caused this space-time diversity of east-west settlement.

**Key words:** subsidence evolution; asymmetric tensile; diversity mechanism; occurrence mechanism; episodic tectonic; Fushan Sag  
**Yu Jianghao,** Key Laboratory of Tectonics and Petroleum Resources of Ministry of Education, China University of Geosciences (Wuhan), Wuhan City, Hubei Province, 430074, China

**Wang Ping, Chang Anding, Dong Anguo et al. Reservoir rock type cluster analysis of Chang<sub>2</sub><sup>1</sup> oil and gas-bearing member, south-east of Ordos Basin. *PGRE*, 2012, 19(5):39–42.**

**Abstract:** Based on the main criteria of terrigenous clastic rock classification and nomenclature at present in China, the clastic fine sandstone-mudstone may be divided into 11 types. Taking core logging into account, especially rock fragment logging and practical lithologic logging interpretation in work, we regard 11 rock type as respective independent object, and formed the object collection, then, after the data treatment and standardization, we count the Chebyshev's distance and implement the cluster analysis, which indicates that, when  $0.2564 < \lambda < 0.4231$ , the 11 rock type of series of fine sandstone-mudstone can be generalized as 5 rock types: mudstone, muddy siltstone, siltstone, silty fine sandstone, fine sandstone. The filed practice of Chang<sub>2</sub><sup>1</sup> oil and gas-bearing member in the south-east of Ordos Basin has proved that the method for rock type classification can both meet the needs of scientific research and field application, it is the optimum selection.

**Key words:** Chang<sub>2</sub><sup>1</sup> oil and gas-bearing member; terrigenous clastic rock; rock type classification; cluster analysis; optimum selection; Ordos Basin

**Wang Ping,** College of Earth Science and Resources, Chang'an University, Xi'an City, Shaanxi Province, 710054, China

**Zhang Liqiang, Yang Wan. Characteristics of red mudstone and its significance in recognition of sequence boundary of Es<sub>4</sub> in Dongying depression. *PGRE*, 2012, 19(5):43–46.**

**Abstract:** In the study of sequence stratigraphy underground, the sequence boundary's identification is mainly based on the seismic section with low vertical resolution, log data with high multiple solution and so on, but ignoring rocks' paleo-weathering characteristic which is relative to unconformable surface. Therefore, it leads to the ambiguity of stratigraphic sequence correlation. Based on the study of petrology, geochemistry and paleo-weathering characteristics about the red mudstone in Es<sub>4</sub> Yong 82 well of Dongying

depression, red mudstone's vertical structure and the relationship with sequence boundary are discussed herein. The mudstone in Es<sub>4</sub> of Yong 82 well mainly includes 4 types: red loose mudstone, red compact massive mudstone, dark grey banding mudstone and grey or grayish purple gypsum mudstone. The red loose mudstone has strong striated rock surface, and its chemical element combinations are close to paleosol. The mudstone's chemical index of alteration analysis indicates that the red loose mudstone has suffered low chemical paleo-weathering, its CIA tends to be lower from top to bottom, indicating rocks' chemical paleo-weathering tends to be lower when the depth increases. The top of the red loose mudstone is relative to the sequence boundary in Es<sub>4</sub>. However, the grey sandstone with red mudstone in the top of early Es<sub>4</sub> should be attributed to upper sequence's low stand system.

**Key words:** Shahejie Formation; mudstone; geochemistry characteristics; sequence boundary; paleosol; Dongying depression  
**Zhang Liqiang**, School of Geoscience, China University of Petroleum (Beijing), Beijing City, 102249, China

**Mu Xing. Seismic weak signal separation based on blind signal processing. *PGRE*, 2012, 19(5):47-49.**

**Abstract:** Blind signal processing technique is one of the hot topics in the field of modern signal processing, aiming at solving problems such as how to separate or estimate the waveforms of the original source from an array of sensors or transducers without or with little knowledge of original waveforms and the characteristics of transmission channels. This paper presents the application of blind signal processing technology to the extraction of seismic weak signals. Based on the investigation and analysis of the relationship between blind signal processing theory and seismic reflection features of subtle pool, an aliasing model of seismic blind-source signals is established in order to extract weak signals from seismic data of target reservoirs. At same time, two new strategies for weak signal extraction are proposed. Using reflection similarity among seismic traces of surrounding rocks and reflection differences of weak signals from target reservoirs, we developed an iterative algorithm for weak signals extraction. The results of simulation and seismic data processing show that the method can extract seismic weak signals successfully and thus improves the resolution of seismic data.

**Key words:** blind signal processing; seismic weak signal; resolution; blind source separation; subtle reservoir

**Mu Xing**, Geoscience Research Institute of Shengli Oilfield Company, SINOPEC, Dongying City, Shandong Province, 257015, China

**Pang Jiandong, Li Sanfu, Jia Cunfu et al. Speed laws and velocity field establishing in ocean deep water area—case of Baiyun sag. *PGRE*, 2012, 19(5):50-53.**

**Abstract:** The complexity of velocity structure in deepwater area leads to distortion of the sedimentary layer structure and the difficulty of depth forecast, and seriously hampered oil and gas exploration of the deepwater area. We analyze characteristics and influencing factors of velocity structure in the Baiyun sag, using AL velocity, VSP velocity, and recognize that there is no necessary relationship between formation velocity and the water depth, and the sedimentary environment essential difference between continental shelf, continental slope deep water area is the fundamental cause of the abnormal rate. Then, we buildup the depth conversion method suitable for the deepwater area of Baiyun sag, by use of the mutual restraint of drilling speed, velocity of coherent inversion and seismic stacking speed. This method resolves tectonic distortion due to rough subsea preferably, and improves depth-prediction accuracy considerably.

**Key words:** slope waters; velocity structure; coherent velocity inversion of pre-stack seismic; time-depth conversion velocity field; Baiyun sag

**Pang Jiandong**, Drilling Engineering Research Institute, CNOOC Energy Technology & Services Limited, Zhanjiang City, Guangdong Province, 524057, China

**Feng Hongxia, Lü Zengwei, Li Shaoxia et al. Influential factor of SP curve in upper Sha4 member, Chunhua oilfield. *PGRE*, 2012, 19(5):54-56.**

**Abstract:** The abnormal phenomena of the data of SP log appeared in the upper Sha4 member in Chunhua oilfield. Some reservoirs have been missed easily and the thickness of some reservoir is inaccurate during the process of identifying reservoir. Based on the theory of SP curve occur, some reasons are analyzed such as formation thickness, formation water salinity and lithological change. The result shows that the abnormal pressure, reservoir thickness, lithology and fluid property caused salt concentration unequal of drilling fluid when the formation was drilled, and this resulted in the anomaly drop of SP curve. In some reservoir, the mud filtrate salinity is more than formation water salinity, this caused SP curve anomaly positive. High carbonate content and microfracture caused by abnormal pressure are the main reasons resulted in SP curve anomaly negative in mudstone. The research obtained good effect in the process of production and improved the accuracy of the logging data interpretation.

**Key words:** upper Sha4 member; reservoir; mudstone; self-potential; diffusion-adsorption electrodynamic potential

**Feng Hongxia**, Shengli Well Logging Company, Dongying City, Shandong Province, 257000, China

**Wang Zhengbo, Ye Yinzhu, Wang Qiang et al. Forecast of remaining oil distribution after polymer flooding by area-split and superposition method. *PGRE*, 2012, 19(5):57-60.**

**Abstract:** Until the end of 2011, oil recovery after polymer flooding is about 53% in China. Residual oil reserves after polymer flooding own pretty high exploitation potential. In order to extract the amount of remaining oil efficiently, it's necessary to study residual oil law and its potential distribution after polymer flooding. For that reason, area-split and superposition method has been put forward specifically, which can be utilized in forecast and studying on residual oil potential distribution of single well and whole reservoir after polymer flooding. Then, the key reservoir in the north of Daqing placanticline is selected as a typical object. After that, the residual oil distribution law of 37 wells after polymer flooding is studied respectively. Finally, based on the changes of recovery